

archives
of thermodynamics

Vol. **38**(2017), No. 3, 3–21

DOI: 10.1515/aoter-2017-0013

The performance of H₂O, R134a, SES36, ethanol, and HFE7100 two-phase closed thermosiphons for varying operating parameters and geometry

RAFAŁ ANDRZEJCZYK*
TOMASZ MUSZYŃSKI

Gdańsk University of Technology, Narutowicza 11/12, 80-233 Gdańsk, Poland

Abstract In this study, the influences of different parameters at performance two-phase closed thermosiphon (TPCT) was presented. It has been confirmed that the working fluid, as well as operating parameters and fill ratio, are very important factors in the performance of TPCT. The article shows characteristics of gravitational tube geometries, as well as the technical characteristic of the most important system components, i.e., the evaporator/condenser. The experiment's plan and the results of it for the two-phase thermosiphon for both evaluated geometries with varying thermal and fluid flow parameters are presented. Experiments were performed for the most perspective working fluids, namely: water, R134a, SES36, ethanol and HFE7100. Obtained research proves the possibility to use TPCT for heat recovery from the industrial waste water.

Keywords: Two-phase closed thermosiphon; Heat pipe; Energy efficiency; NTU (number of heat transfer units); Heat recovery

Nomenclature

A – surface area, m²
 c_p – specific heat, J/kgK
 D – diameter, m

*Corresponding Author. Email rafanrz@pg.gda.pl

f	–	friction factor
\dot{G}	–	mass flux, kg/m ² s
LMTD	–	logarithmic mean temperature difference
L	–	length, m
\dot{m}	–	mass flow, kg/s
NTU	–	number of transfer units
Nu	–	Nusselt number
p	–	pressure, Pa
ΔP	–	pressure drop, Pa
Q	–	heat, J
\dot{Q}	–	rate of heat, W
r	–	radius, m
Re	–	Reynolds number
T	–	temperature, °C
ΔT	–	temperature difference, °C
U	–	overall heat transfer coefficient, W/m ² K
w	–	velocity, m/s
W	–	fluid heat capacity rate, W/K
\dot{V}	–	volumetric flow, m ³ /s
V	–	volume, m ³
X	–	radial direction

Greek symbols

ε	–	heat exchanger effectiveness
φ	–	fill ratio
ρ	–	density of water, kg/m ³
μ	–	dynamic viscosity, Pa s

Superscripts

a	–	adiabatic
abs	–	absolute
c	–	cold
con	–	condensation
e	–	evaporator
exp	–	experimental
h	–	hot
min	–	minimum
max	–	maximum
o	–	outer
out	–	output
p	–	pool boiling
s	–	surface
sh	–	shell
sat	–	saturation
w	–	water



1 Introduction

Thermosiphons are enclosed passive two-phase heat transfer devices. Heat applied to the evaporator section vaporizes the filling liquid which then rises to the condenser section. In the condenser section, vapor condenses and discharges its heat of vaporization. The condensate then flows back to the evaporator section due to gravitational force. The cycle of consecutive evaporation and condensation continues as long as heat is provided at the evaporator and removed at the condenser. The highly efficient thermal transport process of evaporation and condensation maximizes the thermal conductance between the heat source and the heat sink [1]. The amount of heat that can be transported by these devices is normally several orders of magnitude greater than pure conduction through a solid metal [2,3]. They are proven to be very effective, low cost and reliable heat transfer devices for applications in many thermal management and heat recovery systems [4]. They are used in many applications including but not limited to passive ground/road antifreezing [5], baking ovens, heat exchangers in waste heat recovery applications [6], water heaters and solar energy systems and are showing some promise in high-performance electronics thermal management for situations which are orientation specific [7,8]. The heat transfer performance of a two-phase closed thermosiphon (TPCT) is significantly affected by geometry, inclination angle, vapor temperature and pressure, aspect ratio, filling ratio and thermophysical properties of the working fluid. Among those, filling ratio is one of the most important factors [9].

Khazaei [10] investigated TPCT with ethanol as a working fluid. In the experiments, two copper tubes of 1000 mm length and with 15 mm, 25 mm diameters were used. The thermosiphon consisted of three sections, i.e., adiabatic ($L = 160$ mm), evaporating ($L = 430$ mm) and condensing ones ($L = 430$ mm). The heat was supplied by an electric heater. The study showed a good agreement between experimental data and literature correlations for heat transfer coefficient for boiling and condensation into TPCT conditions. The author also proposed own empirical correlation for boiling heat transfer coefficient. Elmosbahi *et al.* [11] investigated the influence of working fluid filling ratio on heat pipe performance, for solar thermal collector applications. Measurements of absorbed heat flux and the temperature in different positions over the heat pipe were done. The heat pipe was made of an 8 mm copper tube (inner diameter was 6 mm). The tube was 715 mm long. The paper proved that the better performance was observed for methanol filling ratio close to 2/3. Fadhl *et al.* [12]

used numerical methods to predict temperature distributions of TPCT. In their work, the volume of the fluid model (VOF) in Ansys Fluent software with user-defined functions was used in calculations. Also, the experimental data from own experimental test section were collected to compare it with numerical simulations. The 0.5 m – a long smooth copper tube with a 22 mm outer diameter was used as a TPCT. The tube wall thickness was 0.9 mm. It consisted of 0.2 m long evaporation section, 0.1 m long adiabatic section, and 0.2 m long condensation section. Into experiments as well as in numerical simulation water was used as a working fluid. The good agreement between experimental data and numerical simulations were obtained. Kannan *et al.* [13] observed the influence of various operational parameters of two-phase closed thermosiphon on its heat transport capability. The three different diameters of thermosiphon tubes were used: 6.7, 9.5 and 12 mm. In all three cases, wall thickness was equal to 0.65 mm. The tubes were 1000 mm long and consisted of 300 mm long evaporation section, 200 mm long adiabatic section, and 500 mm long condensation section. The heat was supplied by means of an electric heater. Condensation section was cooled by water in the simple tube in tube heat exchanger. As working fluids water, ethanol, methanol, and acetone, with filling ratio between 30% to 90% were used. Authors observed marginal influences of filling ratio for heat transfer capabilities. They also observed the best water capabilities to heat transfer for operating temperature between 30 and 70 °C. It has been also emphasized that acetone had the lowest heat transfer capabilities. Jouhara *et al.* [14] carried experimental investigation of small diameter TPCT charged with water and dielectric working fluids: FC-84, FC-77, and FC-3283. The thermosiphon was made out of 200 mm long copper tube with 6 mm inner diameter. The evaporation section was 40 mm long and condensation was 60 mm long. Authors emphasize that the geometrical parameters of TPCT were assumed based on what might be expected in compact heat exchangers. Experiments confirmed the best capabilities to heat transfer for water. Despite the benefits of using dielectric fluid, water outperforms them. Ong *et al.* [15] worked at the power input, filling ratio and angle inclination influence on the thermal performance of two-phase closed thermosiphon. In their study, they used R-410A refrigerant as a working fluid. The tests were performed at a low evaporator temperature. The tested element was fabricated as 930 mm long copper pipe with 12.7 mm outer diameter and 9.5 mm inner diameter. The evaporation, condensation, and adiabatic sections were equally long. As in the

previous studies, the heat was supplied by an electric heater. Condensation section was cooled by tube in tube heat exchanger with water as a coolant. Presented study did not confirm the influence of filling ratio and inclination angle on the TPCT performance. MacGregor *et al.* [16] studied the performance of two-phase thermosiphon with low global warming potential fluids. Authors searched replacements for R134a one of the most common working fluids in such applications. Based on authors selection methodology three potential replacement fluids were chosen, namely water, methanol, and 5% ethylene glycol-water mixture. The mixture of water and glycol was chosen to avoid problems associated with freezing. As a test element, 2200 mm long copper tube with 15.9 mm outer diameter was used. The tube had enhanced internal surface in the form of grooves. The domestic hot and cold water was used as a heat source and heat sink. The experiments showed that water-ethylene glycol mixture could be a good replacement of R134a in TPCT. It should be also noted that for certain conditions its performance was lower than filled with R134a.

The main problem of process industry is to supply efficient heat exchangers for given operating conditions [17–20]. This problem is even more noticeable in waste heat recovery systems [21,22]. The difficulty which occurs during the heat recovery from waste water or industrial water is the contamination, and thereby the risk of infiltration of harmful substances into the heat transfer medium. Another concern is the increase of flow and heat transfer resistance in the context of impurities deposition of on the exchanger surface [23]. In the case of using TPCT, these risks of infiltration of harmful substances into the heat transfer medium are low, also it is quite easy to clean heat transfer surface.

There are not many studies during the two-phase flow of new perspectives dielectric fluids such as HFE-7100, SES36 [24,25]. Those fluids are more environmentally friendly compared to R134a or R404a. In this paper, the thermal performance of copper thermosiphons charged with water as well as ethanol, R134a, HFE-7100, and SES36 is reported for two TPCT geometries. HFE-7100, SES36 liquids were chosen for testing since they are dielectric and cover a range of thermophysical properties, in particular, boiling points in the range of 30–100 °C. Most of the studies emphasize geometries parameters of evaporator and condenser as one of the important factors which influence on TPCT performance. In this studies, the efficiency of condenser heat exchanger was also considered.

2 Experimental apparatus

The measuring system was presented as Fig. 1. The rig consists of two closed loops of test fluid. The facility was intended to work with any non-chemically aggressive working fluids. In both of loops, circulation is forced by electrically powered pumps with a magnetic coupling, capable of providing the mass flow rate from 1×10^{-3} to 5×10^{-3} kg/s and the overpressure up to 800 kPa. This type of pump has been chosen to provide the circulation of fluid in the test sections and to avoid flow pulsations. On the other hand, using distilled water to supply both, the condenser and the evaporator, allowed to eliminate an additional heat conduction resistance associated with sedimentation of the so-called limescale. Adjustment of the mass flow rate is realized by two independent inverters. The inlet and outlet temperatures of hot and cold water were recorded using 4 T-type thermocouples inserted at the inlet and outlet collectors. After obtaining constant parameters, temperatures were measured three times with an accuracy of 0.5°C in the time steps of 20 min, and the average values were used for further analysis. Appropriate arrangements were provided to measure the pressure loss of both pipes in pipe heat exchangers at shell side. Table 1 presented the experimental uncertainty.

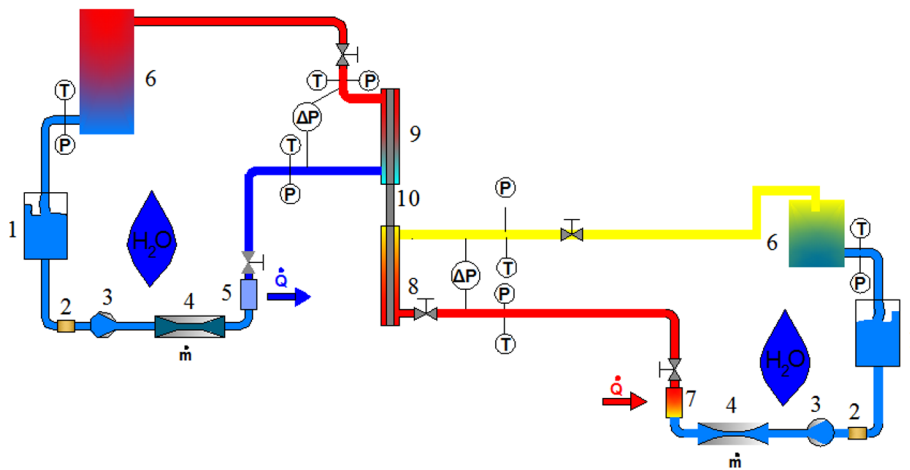


Figure 1: The test rig : 1 – fluid tank, 2 – filter, 3 – pump, 4 – Coriolis flow meter, 5 – chiller, 6 – heat exchanger, 7 – electrical heater, 8 – evaporator, 9 – condenser, 10 – two-phase thermosiphon [26].

Table 1: Partial experimental uncertainties.

Parameter	Unit	Measurement range	Uncertainty
T	°C	10–60	±1.5
\dot{m}_c	kg/s	0.01–0.025	±0,005
ΔP	kPa	0–200	±0.5
P_{abs}	kPa	0–3	±0.108

Experimental uncertainty was determined using the sequential perturbation method of error analysis. This method allows determination of the total experimental error by including errors originating from individual sources into a general database and averaging it using the root mean square method. The error analysis was executed automatically for each data series. It was implemented in the spreadsheets used for data reduction.

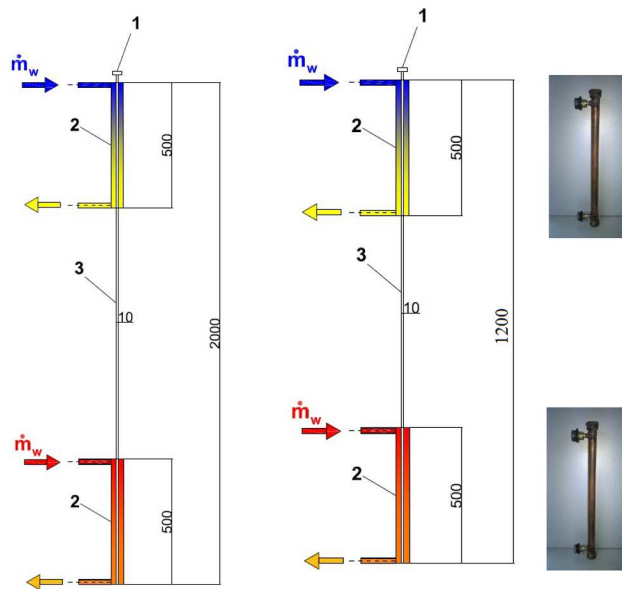


Figure 2: Illustration of two-phase thermosiphons with different length: 1 – Schrodter valve, 2 – typical tube in tube heat exchanger (evaporator/condenser) [26].

The experiments were conducted for two thermosiphon geometries (see Fig. 2). Both investigated elements were made of copper pipes with an inner diameter of 10 mm and outer of 12 mm. In both cases, the length of the section of heat delivery and reception (and therefore also the heat transfer surface) was the same. Due to differences in overall length of the tubes, the length of the adiabatic section varied. Before filling, each thermosiphon was first discharged by the vacuum pump Vi-220SV, whereas before changing the medium, in each case the system was subjected to rinsing, drying and purging with nitrogen, and then emptied in vacuum in order to eliminate the influence of moisture and inert gasses.

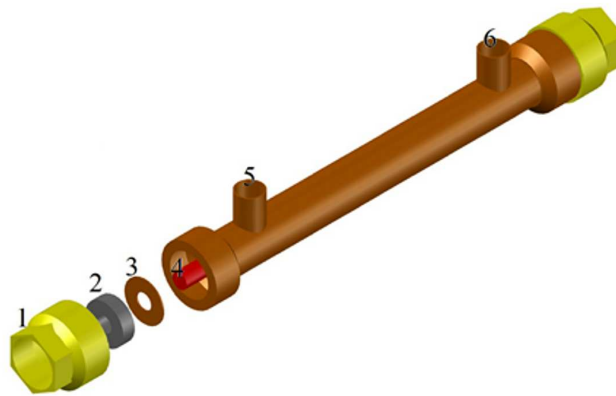


Figure 3: Construction of a typical pipe in pipe heat exchanger working as evaporator/condenser in test elements: 1 – nut, 2 – gasket, 3 – pad, 4 – heat pipe, 5 – inlet, 6 – outlet [26].

The evaporator and condenser were made as a conventional tube in tube heat exchanger (Fig. 3). The shell of the heat exchanger was also made of copper, and the additional Teflon sealing was applied.

3 Experimental research

3.1 Preliminary heat flow tests for tube in tube heat exchangers

Prior to the appropriate experimental measurements of two-phase thermosiphon, preliminary heat-flow tests of tube in tube heat exchanger were carried out. These devices were used to provide/receive heat in the circuit

of the gravitational heat pipe. For this purpose, in the preliminary study, the electric heater was used as a heat source. For the heating element, we have here a case of heat conduction from the internal heat source in the form of a resistance wire powered by electric current.

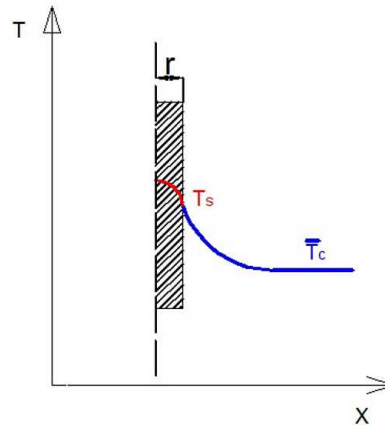


Figure 4: Temperature distribution in double pipe heat exchanger with electrical heat source: \bar{T}_c – mean cold fluid temperature, T_s – wall temperature, r - radius of a heater [26].

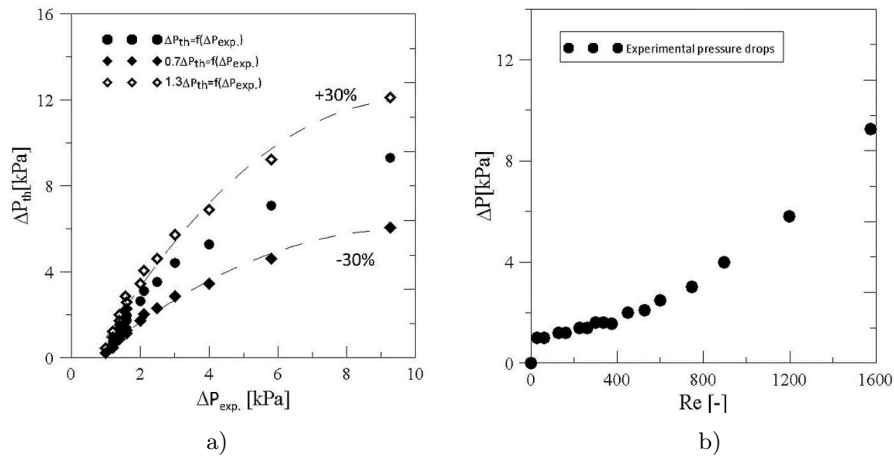


Figure 5: Hydraulic characteristic of water flow in double pipe heat exchanger: a) comparison between experimental and theoretical values of pressure drops, b) pressure drop as a function of Reynolds number.

Figure 5 presents the hydraulic resistance of heat exchangers as a function of Reynolds number. Pressure drop measurement is carried out using the piezoelectric smart differential pressure transducer. The measuring range of the pressure transducer is 0–200 kPa, and the measuring accuracy is $\pm 0.5\%$ of the full scale (FS). The pressure at the inlet and outlet of the heat exchanger is also measured using conventional pressure transducers (measurement is thus duplicated, it is important to verify operation of the system and capture any hardware failure). At the inlet, an absolute pressure transducer with a measuring range of 0–400 kPa and a precision of 0.25% FS is mounted. At the outlet gauge pressure transducer with the range 0–600 kPa and accuracy of 0.5% FS is installed. The experimental results were compared to the theoretical calculations (friction factor was assumed so as for the annular flow $f = 96/\text{Re}$).

$$\Delta P_{th} = 4f \frac{\dot{G}^2}{2\rho}, \quad (1)$$

$$\dot{G} = \frac{\dot{m}_c}{A_p}, \quad (2)$$

$$A_p = \frac{\pi D_e}{4}, \quad (3)$$

$$D_e = \frac{(4V_{sh})}{\pi D_0 L}, \quad (4)$$

$$\text{Re} = \frac{\dot{G} D_e}{\mu}. \quad (5)$$

The outcomes are within the limits of the correlation accuracy and the raised spread of small Reynolds numbers is undoubtedly caused by a measurement equipment errors (± 0.5 kPa).

The efficiency of the heat exchanger was evaluated by using the well-known ε -NTU method. The formulas below presents a calculation methodology:

$$\text{NTU} = \frac{U A}{W_{min}}, \quad (6)$$

$$W_{min} = c_p \dot{m}_c, \quad (7)$$

$$\varepsilon_{exp} = \frac{\dot{Q}}{\dot{Q}_{max}}, \quad (8)$$

$$\dot{Q} = W_c (T_{c,out} - T_{c,in}), \quad (9)$$



$$\Delta T_{max} = T_s - T_{c,in} , \quad (10)$$

$$\dot{Q}_{max} = W_{min} \Delta T_{max} . \quad (11)$$

The predicted value of efficiency was calculated from [27]

$$\varepsilon = \frac{1 - \exp[-NTU(1 - W_{min})]}{1 + W_{min} \exp[-NTU(1 - W_{min})]} \quad \text{for } W_{min} < 1 , \quad (12)$$

and

$$\varepsilon = \frac{NTU}{1 + NTU} \quad \text{for } W_{min} = 1 .$$

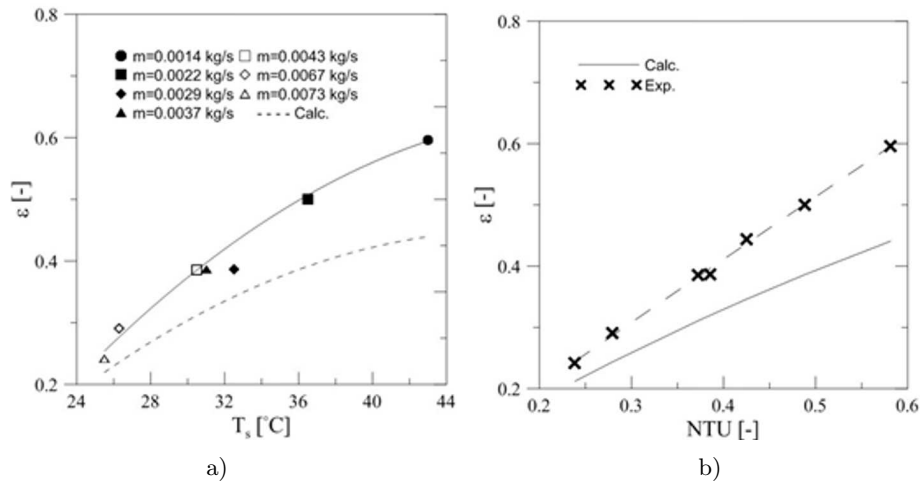


Figure 6: Efficiency of pipe in pipe heat exchanger with variable flow parameters, constant cold inlet water temperature and heat flux of 100 W: a) comparison of experimental and calculated efficiency as a function of surface temperature, b) comparison of experimental and calculated efficiency as a function of NTU [26].

As can be seen from Fig. 6 the heat exchanger efficiency is larger than those predicted by theoretical correlation. It should be also noted that efficiency is increasing proportional to the surface temperature and inversely proportionally to mass flow rate of cooling water. The characteristic lines were formed using regression analysis.

Figure 7 presented results for higher heat flux. There is no significant difference in small water flow rate. However, it has to be emphasized that for larger heat flux efficiency are also increasing for larger water flow rate.

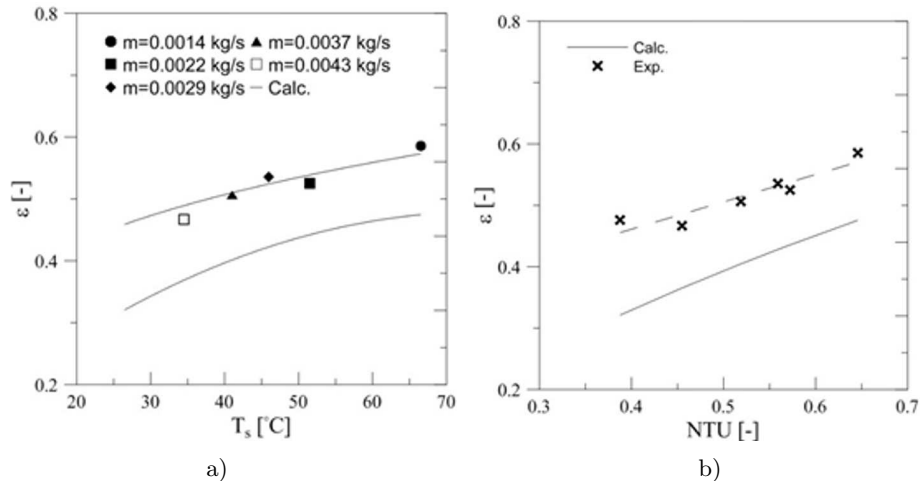


Figure 7: Efficiency of pipe in pipe heat exchanger with variable flow parameters, constant cold water inlet temperature and heat flux of 190 W: a) comparison of experimental and calculated efficiency as a function of surface temperature, b) comparison of experimental and calculated efficiency as a function of NTU [26].

In this case as before the experimental results are greater than calculated. The characteristic curve is much flatter also that curves were formed using regression analysis. The results presented for the steady heat flux prove, that the efficiency of exchanger rise with the wall temperature increase, but only slightly depends on the mass flow rate for greater heat flux. In contrast, for the increasing heat flux, as for constant mass flow rate and the inlet temperature of the cooling water, in the tested heat exchanger efficiency is almost constant (see Fig. 8). In authors opinion, it is an effect of almost constant heat transfer coefficient for the same water mass flow rate.

3.2 Influences of working fluids thermophysical parameters

Obtained results enabled to prepare appropriate ‘strategy’ of experimental studies and proper estimation of set parameters for the target device. The main part this study was is concerned with the selection of appropriate working medium for the application in two-phase thermosiphon, which is an element of the waste heat recovery system. In the study, the following working fluids were used: distilled water, SES36, HFE-07100, R134a, and

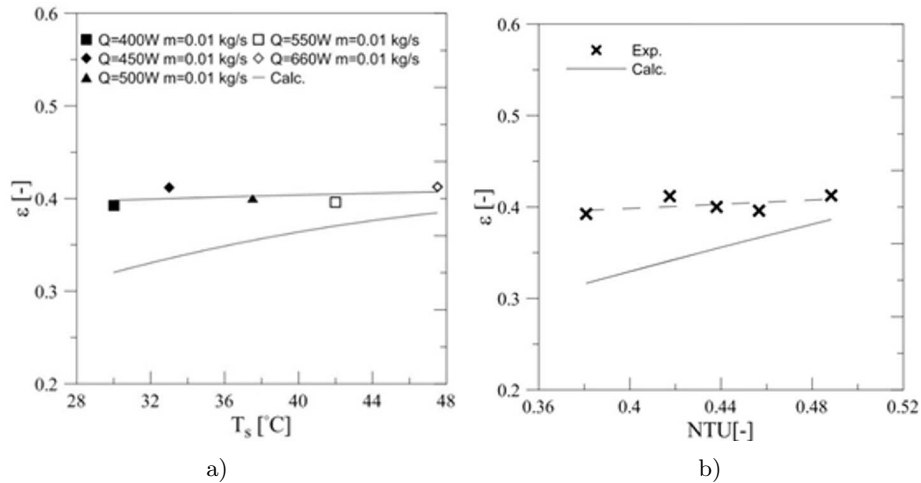


Figure 8: Efficiency of pipe in pipe heat exchanger with constant flow parameters, cold inlet temperature, and variable heat flux: a) comparison of experimental and calculated efficiency as a function of surface temperature, b) comparison of experimental and calculated efficiency as a function of NTU [26].

99,8% ethanol. In Fig. 9 the outcomes are presented (all characteristic curves were formed using regression analysis).

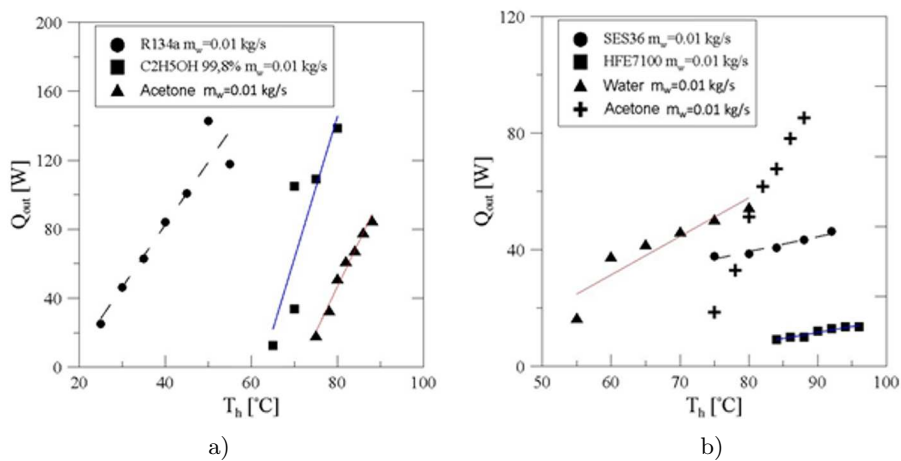


Figure 9: Working characteristic of TPCT for filling ratio of 100% - type 'a' for different fluids but constant flow mass of fluid and pressure: a) most efficient fluids, b) low efficiency fluids.

For the first geometry (type ‘a’) presented results clearly imply that the highest efficiency is for the R134a and ethanol. Wherein the ‘activation temperature’ for R134a is significantly lower than for ethanol. Therefore, this factor should be intended for systems powered by low-temperature heat. The arrangement with ethanol as the working medium is more suitable for recovery heat of temperature above 75 °C. For the second geometry (type ‘b’) following liquids were examined: SES36, water, and ethanol 99.8%. Once again it appeared that a system working with water has a good performance (Fig. 10), but much better results have been obtained with ethanol. On this basis, decision was made to provide a more precise examination of that case. Especially in the context of the results obtained for the previous geometry, above case marked by significantly higher efficiency and lower ‘activation’ temperature.

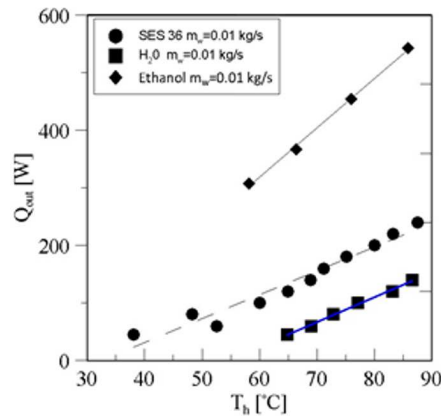


Figure 10: Characteristic of two-phase thermosiphon – type ‘b’ for fill ratio of: 100% – for different fluids but constant cold water mass flow rate and the same operating pressure.

3.3 Influence of filling ratio

The present experimental investigations were extended by varying the filling level in installation (the mass of working fluid), which is defined as a ratio of the volume occupied by the medium, V_p , to the volume of the evaporator, V_e ,

$$\varphi = \frac{V_p}{V_e}. \quad (13)$$

The results were divided into two parts: for filling ratio lower than 80% and above 100% (see Fig. 11).

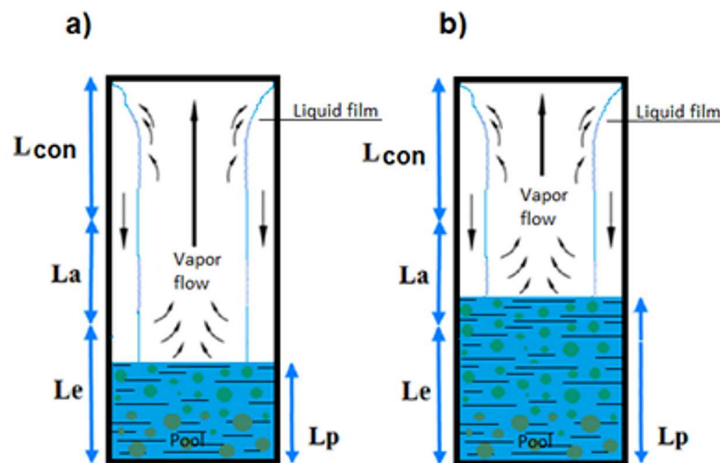


Figure 11: Visualization of flow patterns in TPCT for different fill ratio: a) $\varphi < 80\%$, b) $\varphi > 100\%$ [9].

It can be observed, that for the filling ratio of evaporator below 80%, efficiency reaches its maximum at a rate of heat of approximately 550 W and a flow temperature of the evaporator approx. 80 °C. Another important conclusion is the fact, that the system with the filling of 25% has a considerably better performance at lower temperatures. A smaller amount of fluid in the device leads to its faster evaporation (reduced heat capacity) and thus the soft start of thermosiphon. For the filling ratio of the evaporator above 80% performance of thermosiphon is a linear function of the evaporation temperature. The unit achieves the highest efficiency for the filling in the range of 100–130%. For higher values, an explicit decrease in the performance of the system is noticed.

3.4 Influence of operating parameters at condenser section

Because of the low activation temperature and the largest performance for R134a in the case of type ‘a’ geometry, this fluid was used in the last tests.

The first important proposal is that the saturation temperature of the system rises after reaching the inlet temperature of the hot fluid of approximately 45 °C, then it begins to rapidly decline (see Fig. 13a). The

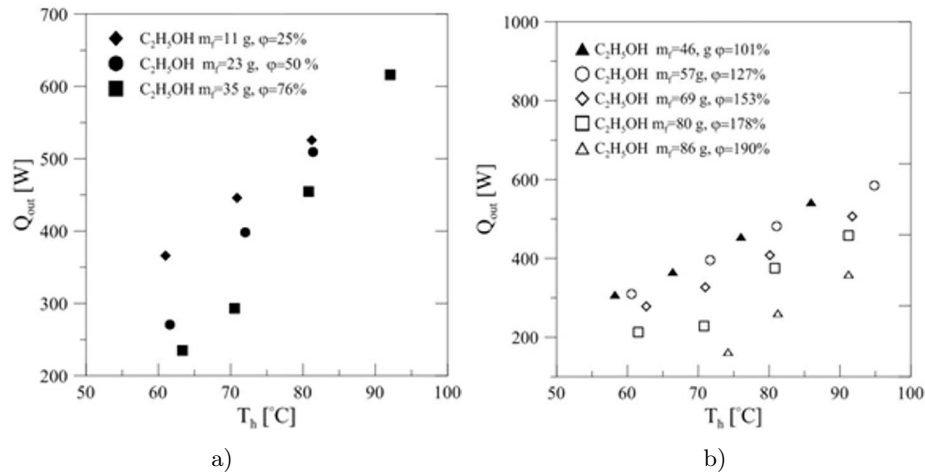


Figure 12: Characteristic of two-phase thermosiphon type 'b' for different filling ratio and constant pressure: a) operation parameter for filling ratio below 70%, b) operation parameters for filling ratio above 70% [26].

decrease is, however, proportional to the mass flow of cooling water. This is in accordance with the characteristics of the condenser. The quantity of receiving heat does not depend on the mass flow of cooling water, but merely on the temperature of the heat source.

4 Summary

The article is a continuation of a previous material devoted to the issue of efficiency of the two-phase thermosiphon in the context of its application in heat recovery systems [6,26]. The work significantly expands prior matter. The paper reviews the basic knowledge about the influence different parameters at TPCT performance. The design of experiment and research methodology is discussed in detail, especially in an effort to stable operation of the system.

The essential case seems to be here the correct approach to adjustment of the efficiency of the condenser. For this reason, the authors conducted autonomous tests on performance and hydraulic characteristics of the double pipe heat exchanger working as an evaporator/condenser. The analysis allowed for appropriate planning of further research.

Relevant studies based on two types of two-phase thermosiphon geometries of different length of the adiabatic section. In both cases, several types

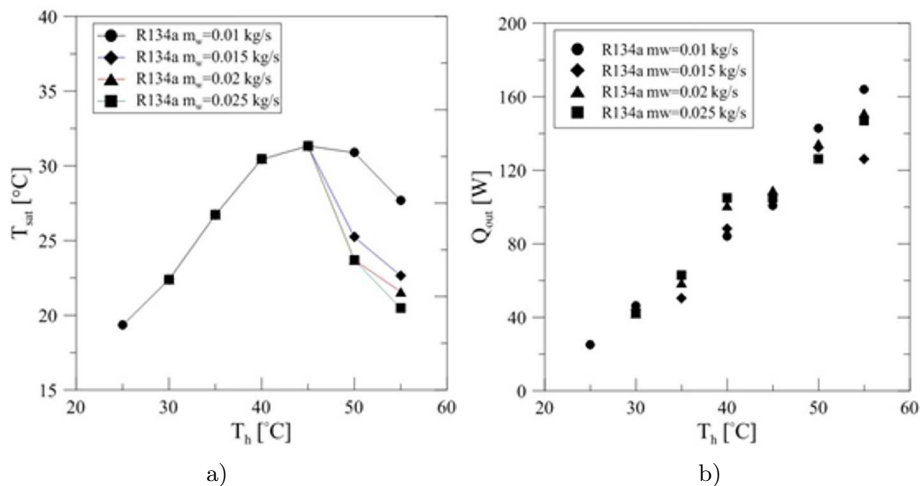


Figure 13: Characteristic of two-phase thermosiphon – type ‘a’ for R134a 100% for fill ratio of: a) influences of hot flow stream (condenser efficiency) for saturation temperature, b) influence of heat source temperature on transferred heat [26]

of working fluid were utilized, including those of inorganic origin – water, organic – ethanol, as well as synthetic R134a and SES36, HFE-7100 belonging to a new ‘family’ of energy fluids.

The best results were obtained for a system working with R134a and ethanol, wherein R134a, due to its properties, operated better in lower evaporation temperatures. The authors also discussed the impact of fill ratio, condenser efficiency on the work of the thermosiphon system.

Received 24 February 2017

References

- [1] BIELIŃSKI H., MIKIELEWICZ J.: *Application of a two-phase thermosyphon loop with minichannels and a minipump in computer cooling*. Arch. Thermodyn. **37**(2016), 1, 3–16, DOI:10.1515/aoter-2016-0001.
- [2] NOIE S.H.: *Heat transfer characteristics of a two-phase closed thermosyphon*. Appl. Therm. Eng. **25**(2005), 495–506.
- [3] REAY D., MCGLEN R., KEW P.: *Heat pipes: Theory, design and applications*. Butterworth-Heinemann, 2013.
- [4] CIEŚLIŃSKI J.T.: *Effect of nanofluid concentration on two-phase thermosyphon heat exchanger performance*. Arch. Thermodyn. **37**(2016), 2, 23–40, DOI:10.1515/aoter-2016-0011.

- [5] ANDRZEJCZYK R., MUSZYŃSKI T., KOZAK P.: *Modern method of snow and ice removal from operational surfaces*. Mater. Bud. **12**(2014), 18–20 (in Polish).
- [6] ANDRZEJCZYK R., MUSZYŃSKI T., KOZAK P.: *Analysis of the effectiveness of waste heat recovery with application of heat pipe. Part I. Structure and operation of the measurement system, design of heat pipe*. Gaz, Woda i Tech. Sanit. (2015) 171–174 (in Polish).
- [7] MUSZYŃSKI T., ANDRZEJCZYK R.: *Heat transfer characteristics of hybrid microjet – Microchannel cooling module*. Appl. Therm. Eng. **93**(2016), 1360–1366, DOI:10.1016/j.applthermaleng.2015.08.085.
- [8] MUSZYŃSKI T., ANDRZEJCZYK R.: *Applicability of arrays of microjet heat transfer correlations to design compact heat exchangers*. Appl. Therm. Eng. **100**(2016), 105–113, DOI:10.1016/j.applthermaleng.2016.01.120.
- [9] JIAO B., QIU L.M., ZHANG X.B., ZHANG Y.: *Investigation on the effect of filling ratio on the steady-state heat transfer performance of a vertical two-phase closed thermosyphon*. Appl. Therm. Eng. **28**(2008), 1417–1426.
- [10] KHAZAEI I.: *Experimental investigation and comparison of heat transfer coefficient of a two phase closed thermosyphon*. Int. J. Energy Environ. **5**(2014), 495–505.
- [11] ELMOSEBAHI M.S., DAHMOUNI A.W., KERKENI C., GUIZANI A.A., BEN NASRALLAH S.: *An experimental investigation on the gravity assisted solar heat pipe under the climatic conditions of Tunisia*. Energy Convers. Manag. **64**(2012), 594–605.
- [12] FADHL B., WROBEL L.C., JOUHARA H.: *Numerical modelling of the temperature distribution in a two-phase closed thermosyphon*. Appl. Therm. Eng. **60**(2013), 122–131.
- [13] KANNAN M., SENTHIL R., BASKARAN R., DEEPANRAJ B.: *An experimental study on heat transport capability of a two phase thermosyphon charged with different working fluids*. Am. J. Appl. Sci. **11**(2014), 584.
- [14] JOUHARA H., ROBINSON A.J.: *Experimental investigation of small diameter two-phase closed thermosyphons charged with water FC-84, FC-77 and FC-3283*. Appl. Therm. Eng. **30**(2010), 201–211.
- [15] ONG K.S., GOH G., TSHAI K.H., CHIN W.M.: *Thermal resistance of a thermosyphon filled with R410A operating at low evaporator temperature*. Appl. Therm. Eng. **106**(2016), 1345–1351, DOI:10.1016/j.applthermaleng.2016.06.080.
- [16] MACGREGOR R.W., KEW P.A., REAY D.A.: *Investigation of low Global Warming Potential working fluids for a closed two-phase thermosyphon*. Appl. Therm. Eng. **51**(2013), 917–925.
- [17] ANDRZEJCZYK R., MUSZYŃSKI T.: *Performance analyses of helical coil heat exchangers. The effect of external coil surface modification on heat exchanger effectiveness*. Arch. Thermodyn. **37**(2016), 4, 137–159. DOI:AOT-00010-2016-0032.
- [18] ANDRZEJCZYK R., MUSZYŃSKI T.: *Thermodynamic and geometrical characteristics of mixed convection heat transfer in the shell and coil tube heat exchanger with baffles*. Appl. Therm. Eng. (2017), DOI:10.1016/j.applthermaleng.2017.04.053.
- [19] ANDRZEJCZYK R., MUSZYŃSKI T., DORAO C.A.: *Experimental investigations on adiabatic frictional pressure drops of R134a during flow in 5mm diameter channel*. Exp. Therm. Fluid Sci. **83**(2017), 78–87, DOI:10.1016/j.expthermflusci.2016.12.016.

- [20] MUSZYŃSKI T., ANDRZEJCZYK R., DORAO C.A.: *Investigations on mixture preparation on two phase adiabatic pressure drop of R134a during flow in 5mm diameter channel*. Arch. Thermodyn. **38**(2017), 3, 99-116, DOI:10.1515/aoter-2017-0018.
- [21] MUSZYŃSKI T., KOZIEL S.M.: *Parametric study of fluid flow and heat transfer over lowered fins of air heat pump evaporator*. Arch. Thermodyn. **37**(2016), 3, 45-62, DOI:10.1515/aoter-2016-0019.
- [22] MUSZYŃSKI T.: *Design and experimental investigations of a cylindrical micro-jet heat exchanger for waste heat recovery systems*. Appl. Therm. Eng. (2017), DOI:10.1016/j.applthermaleng.2017.01.021.
- [23] MA H., YIN L., SHEN X., LU W., SUN Y., ZHANG Y., DENG N.: *Experimental study on heat pipe assisted heat exchanger used for industrial waste heat recovery*. Appl. Energy. **169**(2016), 177-186.
- [24] MIKIELEWICZ D., ANDRZEJCZYK R., MIKIELEWICZ J.: *Pressure Drop of HFE7000 and HFE7100 in Flow Condensation in Minichannels with Account of Non-Adiabatic Effects*. In: MATEC Web Conf., EDP Sciences, 2014, 1007.
- [25] MIKIELEWICZ D., ANDRZEJCZYK R., JAKUBOWSKA B., MIKIELEWICZ J.: *Analytical model with nonadiabatic effects for pressure drop and heat transfer during boiling and condensation flows in conventional channels and minichannels*. Heat Transf. Eng. **37**(2016), 1158-1171.
- [26] ANDRZEJCZYK R., MUSZYŃSKI T.: *Analysis of the effectiveness of waste heat recovery. Part 2. Experimental investigations*. Gaz, Woda I Tech. Sanit. (2016) (in Polish).
- [27] TEKE I., AĞRA Ö., ATAYILMAZ T.Ö., DEMIR H.: *Determining the best type of heat exchangers for heat recovery*. Appl. Therm. Eng. **30**(2010), 577-583.

